ICMIEE20-173

CFD Analysis of Flow Characteristics over Air-Propellers used in a VTOL AquaUAV

Md Rhyhanul Islam Pranto, Md Samiul Hassan Dodul, Mohammad Ilias Inam, Khandkar Aftab Hossain*
Department of Mechanical Engineering, Khulna University of Engineering & Technology, Khulna-9203, BANGLADESH

ABSTRACT
The amphibious (aquatic-aerial) vertical take-off and landing (VTOL) unmanned aerial vehicle simply known as (AquaUAV), a type of aircraft that can travel both in the air and in the underwater, has been seen as a new development to expand UAV's application scenario. It has wide application in the civil and military field, so many institutions have focused on the development of such a vehicle. Achieving a fully operational vehicle capable of aerial and underwater movement is a major challenge due to air-water travel and its stability. As compared to other Amphibious Vehicle designs, a single set of aerial rotors and propellers are used in both air and underwater which will reduce cost, weight and complexity for air to water travel. The aim of the present work is to model a single-layer VTOL AquaUAV and to investigate the fluid flow characteristics for the flow over the air-propellers used in the AquaUAV in air and water domain and to determine the efficient operating RPM for the AquaUAV. In this regard, a comparative investigation is performed using finite volume based CFD simulation to analyze the flow characteristics both in air and water domain. A propeller of 254 mm diameter with five different pitch configurations were tested both in air and water. Thrust forces along with pressure, velocity distributions were determined numerically and plotted to show the feasibility of using the air-propeller in a single-layer AquaUAV model. Numerical results show that the AquaUAV performs efficiently in air near the 4000 RPM range and underwater the efficient RPM is near 300. These results explore a new cross-domain modeling perspective and further improvement in the performance of aquatic-aerial vehicles.

Keywords: AquaUAV, Propeller, CFD, Thrust, RPM.

1. Introduction

Recent advances in aerodynamics theory and micro-controllers have made small Unmanned Aerial Vehicles (UAV) a reality. The small size, low cost and easy maneuverability of these systems have made them potential solutions in avionics industry. Endeavors of growing such vehicles go as far back as World War II when the Soviet Union dealt with a flying submarine project [1]. DARPA (2008) [2] gave a call for proposition for the advancement of a submersible aircraft. The intrigue has additionally developed as automated vehicles have seen a sensational increment in their utilization for civil and military applications. This has boosted the enthusiasm for a stage equipped for air and underwater activity. The amphibious (aquatic-aerial) vertical take-off and landing (VTOL) unmanned aerial vehicle simply known as (AquaUAV), a type of aircraft that can travel both in the air and in the underwater, has been seen as a new development to expand UAV's application scenario. These vehicles are also known by other names like hybrid UAVs, amphibious UAV [3] and unmanned aerial-aquatic vehicle [4]. In this paper AquaUAV is used to define those unmanned vehicles which can fly both in the air and water medium. Numerous advancements to tackle the issues of AquaUAVs are bio-inspired, in light of the fact that numerous creatures can plunge and fly, similar to gannets, flying fish, squids and cormorants [5–10]. There are some various researches on these types of hybrid UAVs. For instance, MIT Lincoln Lab has a hybrid Aerial-Underwater Vehicles(AUVs), which is a little fixed-wing type automated vehicle capable of operating both in air and underwater by folding its wings [11]. Quadcopter UAVs can simply enter and leave the water, however the propellers ought not to contact the water surface. When contacted, the speed is decreased which will make the UAV vulnerable in the water condition. There are two structures to guarantee that AquaUAVs escape from water securely and quickly i.e. two-layer wings setup and single-layer wing setup. Alzubi et al. [12-13] introduced their hybrid quadcopter, known as Loop Copter, equipped with an active buoyancy control framework. However, one inquiry associated with AquaUAVs is that whether the air propellers can be utilized in water conditions. Alzubi et al. [12] proposed a study of using a single set of air propellers in water condition. They have tried a wide scope of pitch for air-propellers that in any case have a similar width and streamlined profile experimentally. The trial results demonstrated that the ethereal propellers can work successfully submerged at low revolution speed (around 180 RPM) without cavitation, giving enough thrust to develop and moving in the water.

This single-layer VTOL quadcopter is the closest to the work presented in this manuscript, it is however in the modeling and simulation phase with a current emphasis on simulating the fluid flow characteristics over the air propellers which will be used in final fabrication. Previous studies don't provide proper information about the propeller aerodynamic characteristics which is the main focus of the study. This study is motivated by need to compliment the limited knowledge about the propeller aerodynamics used in AquaUAVs. For this a CFD approach is used to analyze five

*Corresponding author. Tel.: +8801718025436
E-mail addresses: rhyhanulislam.me21@gmail.com

different pitch air-propeller both in air and water condition numerically. For now, the current goal of this study is to determine the appropriate operating RPM for the AquaUAV both in air and water domain.

2. Methodology

The conceptual model of the AquaUAV is shown in the Fig.1 which will be capable of both air and water operation. It will be a single-layer quadcopter type UAV with active buoyancy control mechanism.

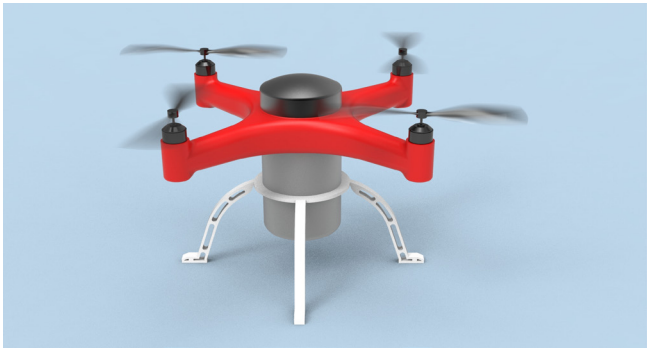

Fig.1 Conceptual model of the proposed AquaUAV

However, the project is now in the modeling and simulation phase with a current emphasis on simulating the fluid flow characteristics over the propellers and to choose the best RPM for optimal operation and prototyping. In this experiment propellers of 254 mm diameter with five different pitch configurations ranging from pitch-4 (101.6 mm) to pitch-6 (152.4 mm) are analyzed. The propellers are designed with the blade element theory technology.

2.1 Computational Method

Propeller shown in the Fig.2 provides information about the propeller dimensions used in the simulation process. The diameter of the propellers is fixed to 254 mm with five different pitches.

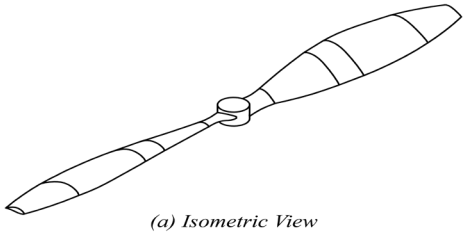

(a) Isometric View

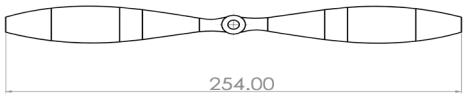

(b) Top view

Fig.2 Propeller Geometry for the AquaUAV

The airfoil used to design the propeller is NACA 4415 airfoil showed in Fig.3 which has a maximum camber of 4% of the cord located 40% of the cord and having a maximum thickness of 15%

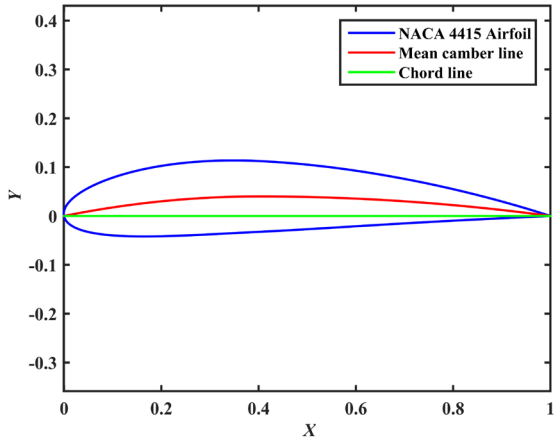

Fig.3 Geometry of the airfoil NACA-4415 used in the AquaUAV propeller

The experiment is done at a fixed Reynolds number (*Re*) of 7×10^5. For this the flow is in turbulent region. So a three dimensional turbulent steady-state solution process is used for the simulation process for both in air and water domain. Standard k-ε viscous model is used to demonstrate the turbulence effect near the propeller walls. The steady-state RANS (Reynolds Average Navier-Stokes) equation is solved using Least squares cell-based gradient system. The RANS equations are time-averaged equations of motion for fluid flow [14].

$$\frac{\partial}{\partial x_i}(\rho u_i) = 0 \tag{1}$$

$$\frac{\partial}{\partial x_j}(\rho u_i u_j) = \frac{\partial p}{\partial x_i} + \frac{\partial}{\partial x_j}[\mu(\frac{\partial u_i}{\partial x_j} + \frac{\partial u_j}{\partial x_i} - \frac{2}{3}\delta_{ij}\frac{\partial u_l}{\partial x_l})] + \frac{\partial}{\partial x_j}(-\rho\overline{u_i' u_j'}) \tag{2}$$

To calculate the thrust value first we have to determine the lift value of propeller element based on the respective RPM; secondly, integrate the lift value of every propeller element along the radius to obtain the total lift of the propeller using the following formula [15]:

$$T = C_T \rho (\frac{N}{60})^2 D^4 \tag{3}$$

And power is calculated from [16]:

$$P = \frac{2\pi N\tau}{60} \quad (4)$$

2.2 Boundary Conditions

The fluid domain is divided into two parts one for linear air flow and other for the rotating propeller. No-slip boundary condition was selected between the interface walls. The inlet was selected as a pressure inlet with a fixed *Re* of $7\times10^{5.}$ The outlet was assumed as pressure outlet. The operating temperature was 298 K in both air and water domain. Both air and water was assumed as working medium with constant density and viscosity respective for air and water. The cell-zone condition at the rotating domain was set to frame motion with constant RPM ranging from 1000-10,000 for air and 100-500 for water domain.

2.3 Mesh Generation and Wall Treatment:

The tetrahedral mesh was created for better convergence and control of the wall function, shown in Fig.4. The inflation was set to 1.20 near the propeller walls and growth rate 1.05 with high smoothing and finer relevance center for better mesh quality. For the mesh curvature size function was implemented with a minimum element size of 0.001 mm and curvature angle of 18°. The maximum y^+ value for the mesh near the propeller geometry was about 170 which is well in the effectiveness range (30-300) for k-ε turbulence model[17].

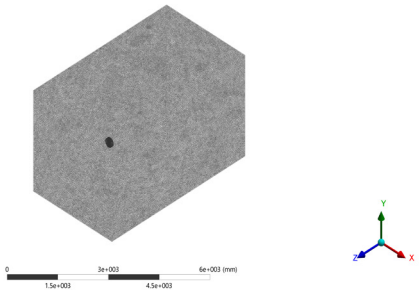

(a)

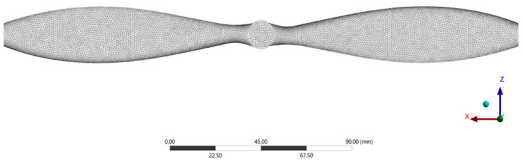

(b)

Fig.4 Mesh of the *(a)* fluid-domain and *(b)* propeller

2.4 Grid Independence Test

Table 1 Grid independence test results for the computational domain for pitch-4 propeller

Number of Elements	Thrust Force (N)
6.714×10^5	1.85
9.378×10^5	1.96
1.380×10^6	2.04
2.241×10^6	2.19
3.147×10^6	2.23
4.178×10^6	2.23
6.935×10^6	2.23

A series of simulations were performed to find the mesh independent solutions for the fluid domain. Mesh containing 3.147×10^6 number of elements was selected for further simulation process for pitch-4 propeller. The other fluid domain meshes were also generated with the same mesh configuration and founded with the similar mesh quality for each propeller later.

3. Results & Discussion:

Fig.5-*(a)* and *(b)* depict the total thrust force generated by the propellers in air and water domain. From the figures we can see that the thrust force increases both in air and water domain with the increase of operating RPM. In both operating regions the maximum thrust force is generated by the pitch-6 propeller and minimum by the pitch-4 propeller. For example, the maximum thrust generated by pitch-4 propeller at 5000 RPM is 3.56N and the thrust generated by pitch-6 propeller at the same RPM is 4.75N which is 33.43% higher than the pitch-4 propeller thrust.

Fig.6-*(a)* and *(b)* demonstrate the power consumption for the propellers to rotate at a certain RPM in air and water domain respectively. The figures show that as the RPM increases the power consumption rate also increases. The highest power consumed by the propeller is 327.53 Watts in air operation for pitch-6 propeller in order to rotate at 10,000 RPM. And in water the height power consumed by the pitch-6 propeller is 32.96 Watts for rotating in 500 RPM. It is seen that the power required for underwater operation is much lesser than air operation.

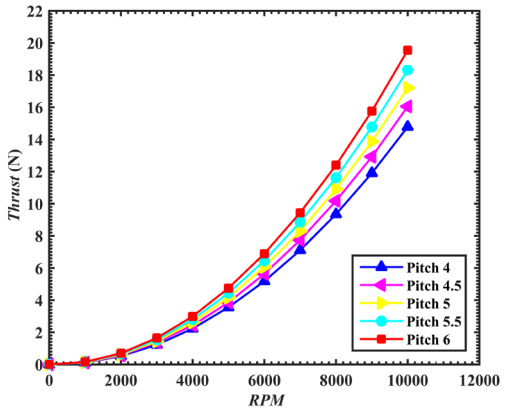

(a)

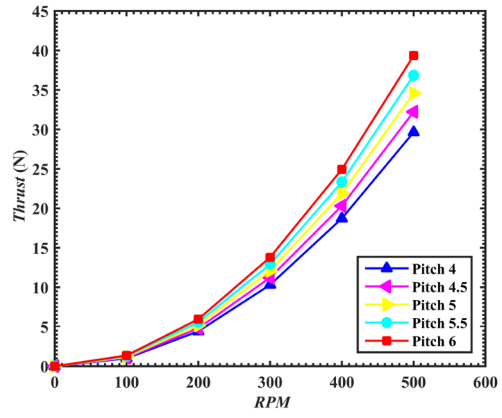

(b)

Fig.5 Thrust force generated by the propellers in the *(a)* air and *(b)* water domain

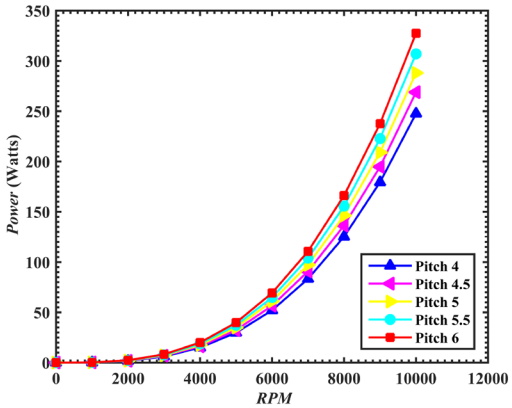

(a)

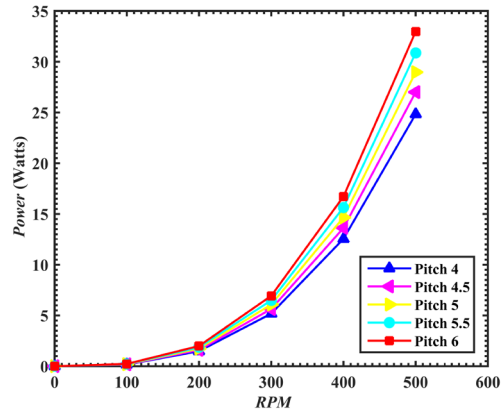

(b)

Fig.6 Power consumed by propellers in the in the *(a)* air and *(b)* water domain

Although it is shown by Fig.5 that with the increase of the propeller RPM the thrust force increases. But on the other hand it requires more power to operate in higher RPM. For instance, to rotate in 10,000 RPM, pitch-5 propeller needs 288.14 Watts of power to generate 18.32N thrust force, which is not efficient for the operation of the AquaUAV. In order to determine the effective RPM for efficient operation the thrust to power ratio is calculated.

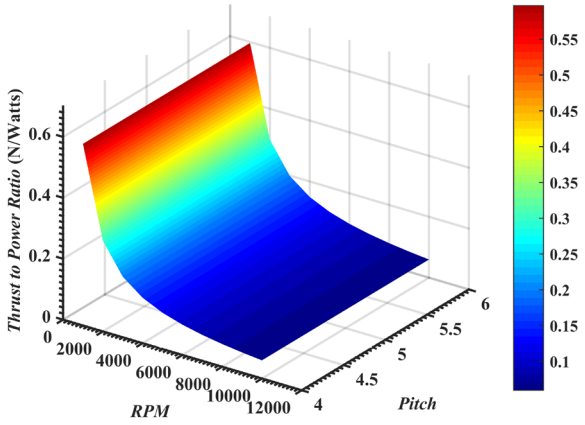

(a)

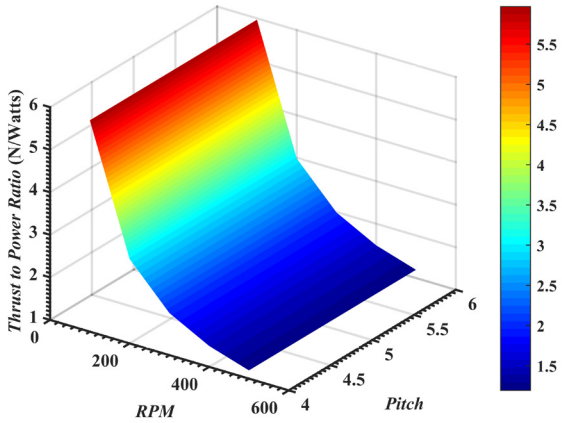

(b)

Fig.7 Thrust to Power ratio of the propellers with respect to RPM and pitch in *(a)* air and *(b)* water domain.

Fig.7-*(a)* and *(b)* depict the information about thrust to power ratio for the propellers with respect to RPM and propeller pitch. The figures show that with the increase of RPM the thrust to power ratio decreases for all propellers. It was seen before that with higher RPM the thrust force increased but it required a much higher power consumption which isn't efficient at all. From the Fig.7-*(a)* we can see that the thrust to power ratio decreases which indicates how efficiently the power is utilized to produce lift. Higher thrust to power ratio indicates higher efficiency. The highest thrust to power ratio is found in the lower RPM condition but in that case the thrust produced isn't enough for the maneuverability of the AquaUAV in both air and water

condition. But after 4000 RPM the thrust to power ratio change is negligible which indicates it won't perform efficiently after 4000 RPM in the air domain because it will require enormous power input to produce thrust at that RPM. Similarly, from the Fig.7-*(b)* it can be seen that the same condition applies for the propellers in water domain. The decrease in thrust to power ratio is much lesser after 300 RPM. So the efficient operating RPM in underwater condition would be around 300.

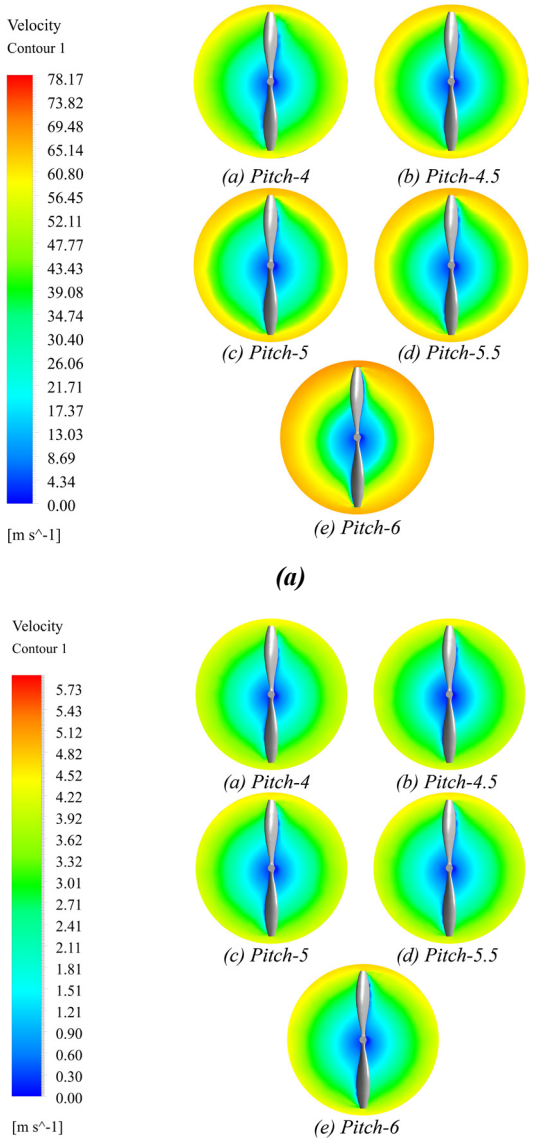

Fig.8 Velocity contours for the propellers at 4000 RPM in *(a)* air and 300 RPM in *(b)* water domain

Fig.8-*(a)* and *(b)* show the velocity contours for the propellers in air at 4000 RPM and at 300 RPM underwater. It can be seen from the figures that the velocity at the propeller tips are higher than the other regions. The stagnation condition occurs at the center of the propellers. It is also seen that as the pitch increases the velocity also increases. For example, the maximum velocity is for pitch-6 propeller of 78.17 m/s at the propeller tip in air domain.

Fig.9-*(a)* and *(b)* demonstrate the pressure contours for the propellers at 4000 RPM in air operation and 300 RPM in underwater condition. From the pressure contours it can be seen that the pressure distribution is higher at the leading surfaces of the propellers and lower at the tips as flow separation occurs at the tip region. Pitch-6 propeller has the highest pressure distribution than other propellers with a maximum pressure impact of 332.82 Pa at the leading edge in air at 4000 RPM.

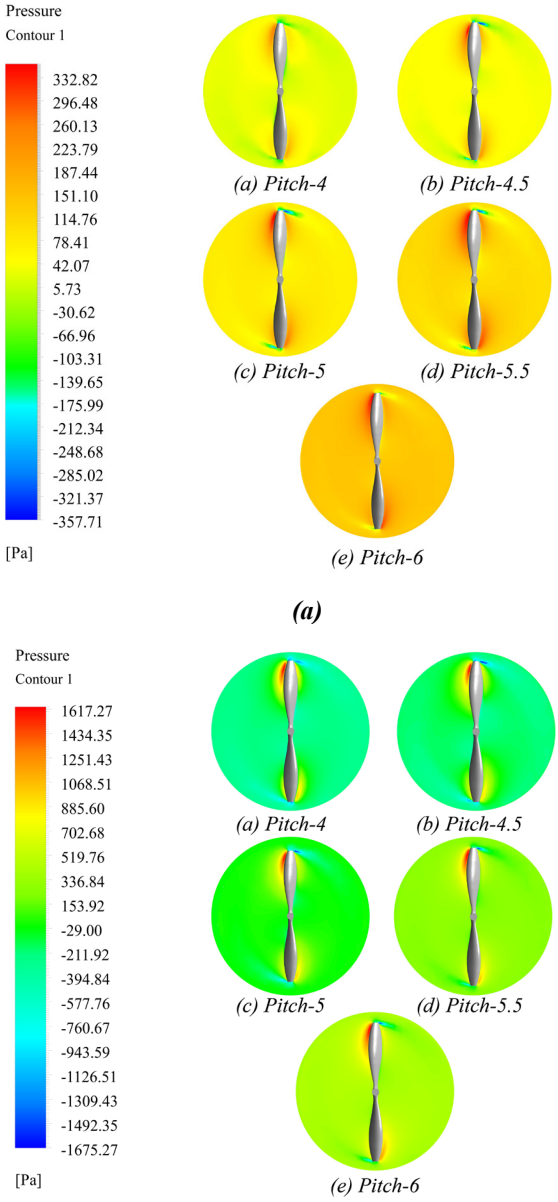

Fig.9 Pressure contours for the propellers at 4000 RPM in *(a)* air and 300 RPM in *(b)* water domain

4. Conclusion

In this paper, the flow characteristics for the AquaUAV propellers have been studied. A steady-state solution approached is used to solve the problem with commercial CFD package Ansys FLUENT 18.1. This paper proposed the feasibility of using aerial propellers in underwater condition using fluid flow simulation process. We have tested a wide range of pitched propeller with a fixed diameter with the same aerodynamic profile. The results show that the air-propellers also performed efficiently in underwater condition at low rotational speed around 300 RPM providing enough thrust for maneuverability in the water. The efficient operating condition for air operation was also determined with a RPM around 4000. This aerodynamic analysis will certainly help the ongoing development of the AquaUAV.

References

[1] P. Marks, From sea to sky: Submarines that fly, New Sci. 207 (2010) 32–35.

[2] DARPA. Broad Agency Announcement: Submersible Aircraft. DARPA-BAA-09-06. 2008., (n.d.).

[3] G. Pisanich, S. Morris, Fielding an amphibious UAV: development, results, and lessons learned, in: Proceedings. 21st Digit. Avion. Syst. Conf., IEEE, 2002: pp. 8C4-8C4.

[4] J. Moore, A. Fein, W. Setzler, Design and analysis of a fixed-wing unmanned aerial-aquatic vehicle, in: 2018 IEEE Int. Conf. Robot. Autom., IEEE, 2018: pp. 1236–1243.

[5] Y. Bar-Cohen, Biomimetics—using nature to inspire human innovation, Bioinspir. Biomim. 1 (2006) P1.

[6] B. Bhushan, Biomimetics: lessons from nature–an overview, (2009).

[7] Vincent JF (2009) Biomimetics--a review. Proc Inst Mech Eng H 223(8): 919-939., (n.d.).

[8] N.F. Lepora, P. Verschure, T.J. Prescott, The state of the art in biomimetics, Bioinspir. Biomim. 8 (2013) 13001.

[9] L. Ren, Y. Liang, Preliminary studies on the basic factors of bionics, Sci. China Technol. Sci. 57 (2014) 520–530.

[10] T.G. Hou, X.B. Yang, T.M. Wang, J.H. Liang, S.W. Li, Y.B. Fan, Locomotor transition: how squid jet from water to air, Bioinspir. Biomim. 15 (2020) 36014. https://doi.org/10.1088/1748-3190/ab784b.

[11] A. Fabian, Y. Feng, E. Swartz, D. Thurmer, R. Wang, Hybrid Aerial Underwater Vehicle (MIT Lincoln Lab), (2012).

[12] H. Alzu'bi, O. Akinsanya, N. Kaja, I. Mansour, O. Rawashdeh, Evaluation of an aerial quadcopter power-plant for underwater operation, in: 2015 10th Int. Symp. Mechatronics Its Appl., IEEE, 2015: pp. 1–4.

[13] H. Alzu'bi, I. Mansour, O. Rawashdeh, Loon copter: Implementation of a hybrid unmanned aquatic–aerial quadcopter with active buoyancy control, J. F. Robot. 35 (2018) 764–778.

[14] B.E. Launder, First steps in modelling turbulence and its origins: A commentary on Reynolds (1895) "On the dynamical theory of incompressible viscous fluids and the determination of the criterion," Philos. Trans. R. Soc. A Math. Phys. Eng. Sci. (2015). https://doi.org/10.1098/rsta.2014.0231.

[15] Liu Peiqing. Theory and application of air propeller. [M]. Beijing, Beijing University of Aeronautics and Astronautics Press, 2005:42-46, (n.d.).

[16] S.H. Loewenthal, Design of power-transmitting shifts, (1984).

[17] H.K. Versteeg, W. Malalasekera, Computational fluid dynamics, Finite Vol. Method. (1995).

Nomenclature

ρ : Density, kg/m^3
u : Velocity, m/s
k : Kinematic viscosity, kg/m-s
T : Thrust Force, N
C_T : Coefficient of Thrust
N : Rotational Speed, RPM
D : Diameter, m
P : Power, Watts
τ : Torque, N.m